



KEK preprint 2002-17

Belle preprint 2002-11

Measurements of Branching Fractions and Decay Amplitudes in $B \rightarrow J/\psi K^*$ decays

K. Abe⁹, K. Abe⁴³, T. Abe⁴⁴, I. Adachi⁹, Byoung Sup Ahn¹⁶, H. Aihara⁴⁵,
M. Akatsu²³, Y. Asano⁵⁰, T. Aso⁴⁹, V. Aulchenko², T. Aushev¹³,
A. M. Bakich⁴⁰, Y. Ban³⁴, E. Banas²⁸, A. Bay¹⁹, P. K. Behera⁵¹, A. Bondar²,
A. Bozek²⁸, T. E. Browder⁸, B. C. K. Casey⁸, Y. Chao²⁷, B. G. Cheon³⁹,
R. Chistov¹³, S.-K. Choi⁷, Y. Choi³⁹, M. Danilov¹³, L. Y. Dong¹¹,
S. Eidelman², V. Eiges¹³, Y. Enari²³, F. Fang⁸, C. Fukunaga⁴⁷, T. Gershon⁹,
K. Gotow⁵², R. Guo²⁵, J. Haba⁹, K. Hanagaki³⁵, T. Hara³², H. Hayashii²⁴,
M. Hazumi⁹, E. M. Heenan²², I. Higuchi⁴⁴, T. Higuchi⁴⁵, T. Hokuue²³,
Y. Hoshi⁴³, S. R. Hou²⁷, W.-S. Hou²⁷, H.-C. Huang²⁷, T. Igaki²³, T. Iijima²³,
K. Inami²³, A. Ishikawa²³, H. Ishino⁴⁶, R. Itoh⁹, M. Iwamoto³, H. Iwasaki⁹,
Y. Iwasaki⁹, P. Jalocha²⁸, J. H. Kang⁵⁴, J. S. Kang¹⁶, P. Kapusta²⁸,
S. U. Kataoka²⁴, N. Katayama⁹, H. Kawai³, Y. Kawakami²³, N. Kawamura¹,
T. Kawasaki³⁰, H. Kichimi⁹, D. W. Kim³⁹, Heejong Kim⁵⁴, H. J. Kim⁵⁴,
H. O. Kim³⁹, Hyunwoo Kim¹⁶, K. Kinoshita⁵, S. Korpar^{21,14}, P. Križan^{20,14},
P. Krokovny², R. Kulasiri⁵, S. Kumar³³, Y.-J. Kwon⁵⁴, J. S. Lange^{6,36},
G. Leder¹², S. H. Lee³⁸, D. Liventsev¹³, J. MacNaughton¹², G. Majumder⁴¹,
T. Matsui²³, S. Matsumoto⁴, T. Matsumoto^{23,47}, W. Mitaroff¹²,
K. Miyabayashi²⁴, Y. Miyabayashi²³, H. Miyake³², H. Miyata³⁰,
G. R. Moloney²², S. Mori⁵⁰, T. Mori⁴, T. Nagamine⁴⁴, Y. Nagasaka¹⁰,
T. Nakadaira⁴⁵, E. Nakano³¹, M. Nakao⁹, J. W. Nam³⁹, Z. Natkaniec²⁸,
S. Nishida¹⁷, O. Nitoh⁴⁸, T. Nozaki⁹, S. Ogawa⁴², F. Ohno⁴⁶, T. Ohshima²³,
T. Okabe²³, S. Okuno¹⁵, S. L. Olsen⁸, W. Ostrowicz²⁸, H. Ozaki⁹,
P. Pakhlov¹³, H. Palka²⁸, C. W. Park¹⁶, H. Park¹⁸, K. S. Park³⁹,
L. E. Piilonen⁵², M. Rozanska²⁸, K. Rybicki²⁸, H. Sagawa⁹, S. Saitoh⁹,
Y. Sakai⁹, M. Satapathy⁵¹, A. Satpathy^{9,5}, O. Schneider¹⁹, S. Schrenk⁵,
S. Semenov¹³, K. Senyo²³, R. Seuster⁸, M. E. Sevier²², H. Shibuya⁴²,
B. Shwartz², V. Sidorov², J. B. Singh³³, S. Stanić^{50,*}, A. Sugi²³,
A. Sugiyama²³, K. Sumisawa⁹, T. Sumiyoshi^{9,47}, K. Suzuki⁹, S. Suzuki⁵³,
S. Y. Suzuki⁹, T. Takahashi³¹, F. Takasaki⁹, N. Tamura³⁰, M. Tanaka⁹,
G. N. Taylor²², Y. Teramoto³¹, S. Tokuda²³, M. Tomoto⁹, T. Tomura⁴⁵,
S. N. Tovey²², K. Trabelsi⁸, T. Tsuboyama⁹, T. Tsukamoto⁹, S. Uehara⁹,

S. Uno⁹, S. E. Vahsen³⁵, G. Varner⁸, K. E. Varvell⁴⁰, C. H. Wang²⁶,
J. G. Wang⁵², M.-Z. Wang²⁷, Y. Watanabe⁴⁶, E. Won³⁸, B. D. Yabsley⁵²,
Y. Yamada⁹, A. Yamaguchi⁴⁴, Y. Yamashita²⁹, M. Yamauchi⁹,
M. Yokoyama⁴⁵, K. Yoshida²³, Y. Yuan¹¹, Y. Yusa⁴⁴, J. Zhang⁵⁰,
Z. P. Zhang³⁷, V. Zhilich², Z. M. Zhu³⁴, and D. Žontar⁵⁰

(The Belle Collaboration)

- ¹Aomori University, Aomori
- ²Budker Institute of Nuclear Physics, Novosibirsk
- ³Chiba University, Chiba
- ⁴Chuo University, Tokyo
- ⁵University of Cincinnati, Cincinnati OH
- ⁶University of Frankfurt, Frankfurt
- ⁷Gyeongsang National University, Chinju
- ⁸University of Hawaii, Honolulu HI
- ⁹High Energy Accelerator Research Organization (KEK), Tsukuba
- ¹⁰Hiroshima Institute of Technology, Hiroshima
- ¹¹Institute of High Energy Physics, Chinese Academy of Sciences, Beijing
- ¹²Institute of High Energy Physics, Vienna
- ¹³Institute for Theoretical and Experimental Physics, Moscow
- ¹⁴J. Stefan Institute, Ljubljana
- ¹⁵Kanagawa University, Yokohama
- ¹⁶Korea University, Seoul
- ¹⁷Kyoto University, Kyoto
- ¹⁸Kyungpook National University, Taegu
- ¹⁹Institut de Physique des Hautes Énergies, Université de Lausanne, Lausanne
- ²⁰University of Ljubljana, Ljubljana
- ²¹University of Maribor, Maribor
- ²²University of Melbourne, Victoria
- ²³Nagoya University, Nagoya
- ²⁴Nara Women's University, Nara
- ²⁵National Kaohsiung Normal University, Kaohsiung
- ²⁶National Lien-Ho Institute of Technology, Miao Li
- ²⁷National Taiwan University, Taipei
- ²⁸H. Niewodniczanski Institute of Nuclear Physics, Krakow
- ²⁹Nihon Dental College, Niigata
- ³⁰Niigata University, Niigata
- ³¹Osaka City University, Osaka
- ³²Osaka University, Osaka
- ³³Panjab University, Chandigarh
- ³⁴Peking University, Beijing
- ³⁵Princeton University, Princeton NJ
- ³⁶RIKEN BNL Research Center, Brookhaven NY
- ³⁷University of Science and Technology of China, Hefei
- ³⁸Seoul National University, Seoul
- ³⁹Sungkyunkwan University, Suwon

⁴⁰University of Sydney, Sydney NSW
⁴¹Tata Institute of Fundamental Research, Bombay
⁴²Toho University, Funabashi
⁴³Tohoku Gakuin University, Tagajo
⁴⁴Tohoku University, Sendai
⁴⁵University of Tokyo, Tokyo
⁴⁶Tokyo Institute of Technology, Tokyo
⁴⁷Tokyo Metropolitan University, Tokyo
⁴⁸Tokyo University of Agriculture and Technology, Tokyo
⁴⁹Toyama National College of Maritime Technology, Toyama
⁵⁰University of Tsukuba, Tsukuba
⁵¹Utkal University, Bhubaneswer
⁵²Virginia Polytechnic Institute and State University, Blacksburg VA
⁵³Yokkaichi University, Yokkaichi
⁵⁴Yonsei University, Seoul
 *on leave from Nova Gorica Polytechnic, Slovenia

Abstract

The branching fractions and the decay amplitudes of $B \rightarrow J/\psi K^*$ decays are measured in a 29.4 fb^{-1} data sample collected with the Belle detector at the KEKB electron-positron collider. The decay amplitudes of helicity states of the $J/\psi K^*$ system are determined from the full angular distribution of the final state particles in the transversity basis. The branching fractions are measured to be $(1.29 \pm 0.05 \pm 0.13) \times 10^{-3}$ for neutral mesons and $(1.28 \pm 0.07 \pm 0.14) \times 10^{-3}$ for charged mesons. The measured longitudinal and transverse (perpendicular to the transversity plane) amplitudes are $|A_0|^2 = 0.62 \pm 0.02 \pm 0.03$ and $|A_\perp|^2 = 0.19 \pm 0.02 \pm 0.03$, respectively. The value of $|A_\perp|^2$ shows that the CP even component dominates in the $B^0 \rightarrow J/\psi K^{*0}(K_S \pi^0)$ decay.

PACS: 13.25.Hq, 14.40.Nd

1 Introduction

The decay $B^0 \rightarrow J/\psi K^{*0} (K^{*0} \rightarrow K_S \pi^0)$ has the same quark level diagram as $B^0 \rightarrow J/\psi K_S$ and may, therefore, be used for a determination of the CP violation parameter $\sin 2\phi_1$. However, since the $J/\psi K^*$ system has three possible helicity states with different superpositions of CP eigenstates, the dilution of the CP asymmetry depends on the degree of polarization of the decay. The mix of CP even and odd states must be known before a measurement of $\sin 2\phi_1$ can be attempted.

The CP mix can be determined through a full angular analysis of the final state particles to obtain the decay amplitudes of the system in the transversity basis. Once the CP mix is measured, the CP eigenstates of the events may be projected out in a statistical way. The full angular analysis also serves as a test of the factorization hypothesis by measuring the imaginary part of the decay amplitudes.

In this paper, we report the measurements of branching fractions for $B^0 \rightarrow J/\psi K^{*0}$ and $B^+ \rightarrow J/\psi K^{*+}$ and the decay amplitudes of the system obtained by a full three-dimensional angular analysis. The determination of $\sin 2\phi_1$ based on the reconstruction of these decays is described elsewhere[1].

2 Data sample

The data sample used in this analysis corresponds to an integrated luminosity of 29.4 fb^{-1} recorded with the Belle detector[2] at the KEKB electron-positron collider[3]. Events are required to satisfy the hadronic event selection criteria[1] and have $R_2 < 0.5$, where R_2 is the ratio of the second to zeroth Fox-Wolfman parameters[4].

The branching fractions and decay amplitudes are measured by reconstructing neutral and charged B mesons in $B^0 \rightarrow J/\psi K^{*0}$ and $B^+ \rightarrow J/\psi K^{*+}$ (inclusion of charge conjugate modes is implied throughout this paper). The reconstruction of the J/ψ is performed using the dilepton decays, $J/\psi \rightarrow e^+e^-$ and $\mu^+\mu^-$. For the e^+e^- mode, electrons and positrons are identified by matching between the energy measured in the electromagnetic calorimeter (ECL) and the momentum measured in the central drift chamber (CDC), the shape of the cluster energy deposit in the ECL, the dE/dx measured in the CDC, and the light yield in the aerogel Čerenkov counters (ACC). A likelihood is calculated from these measurements and required to be consistent with the electron hypothesis. To correct for energy lost by final state radiation, the energy of any cluster in the ECL within 0.05 radians of the track momentum is added

to that of the track. The invariant mass of each pair of identified electrons is calculated, and the pair is identified as $J/\psi \rightarrow e^+e^-$ if the mass is in the range $2.95 \text{ GeV}/c^2 < M(e^+e^-) < 3.15 \text{ GeV}/c^2$. Tracks are identified as muons by means of a likelihood number based on (i) a comparison of the number of layers with associated hits in the muon detector (KLM) with the number expected based on momentum and (ii) the energy of the associated hit in the ECL. An oppositely charged pair of identified muons is identified as $J/\psi \rightarrow \mu^+\mu^-$ if the invariant mass is in the range $3.05 \text{ GeV}/c^2 < M(\mu^+\mu^-) < 3.15 \text{ GeV}/c^2$. To improve the momentum resolution, a kinematic fit which uses the J/ψ mass as a constraint is performed on J/ψ candidates passing the above selections.

K^{*0} and K^{*+} candidates are reconstructed in the decay modes $K^{*0} \rightarrow K^+\pi^-$, $K^{*+} \rightarrow K_S\pi^+$, $K^{*+} \rightarrow K^+\pi^0$, and $K^{*0} \rightarrow K_S\pi^0$. Charged kaons are identified by requiring the kaon likelihood of a track to be consistent with expectations. The kaon likelihood is obtained by combining measurements of the time of flight measured by the scintillation counters (TOF), dE/dx by the CDC and the hit information in the ACC. Tracks which are not identified as kaons and not used as leptons in the J/ψ reconstruction are treated as charged pion candidates. K_S candidates are reconstructed from pairs of oppositely charged tracks which satisfy three conditions: 1) the distance of the closest approach of both tracks to the nominal interaction point is larger than 0.03 cm, 2) the angle between the K_S momentum vector and the vector displacement of the K_S vertex point from the J/ψ vertex is less than 0.15 radians, and 3) the reconstructed decay vertex of the K_S is at least 0.1 cm away from the interaction point. Each pair with invariant mass satisfying $0.47 \text{ GeV}/c^2 < M(\pi^+\pi^-) < 0.52 \text{ GeV}/c^2$ is identified as a K_S . To improve the mass resolution the momenta are re-fitted, constraining both tracks to originate at the reconstructed vertex. Candidate π^0 mesons are reconstructed from clusters in the ECL that are unmatched to charged tracks and have energy greater than 40 MeV. A photon pair with an invariant mass in the range $0.125 \text{ GeV}/c^2 < M(\gamma\gamma) < 0.145 \text{ GeV}/c^2$ is identified as a π^0 . A mass-constrained fit is performed to obtain the momentum of the π^0 . A K^* is identified if the absolute difference between the invariant mass of an identified $K\pi$ pair and the nominal $K^*(892)$ mass is less than $75 \text{ MeV}/c^2$.

3 Measurement of branching fractions

Candidate B^0 and B^+ mesons are reconstructed by selecting events with a J/ψ and a K^* and examining two quantities in the center-of-mass of the $\Upsilon(4S)$, the beam-constrained mass (M_{bc}) and the energy difference between the B candidate and the beam energy (ΔE). The beam-constrained mass, which is the invariant mass of a reconstructed J/ψ and K^* calculated taking the energy to be the beam energy, is required to be in the range $5.20 - 5.29 \text{ GeV}/c^2$. For

modes with charged tracks only, $|\Delta E|$ is required to be less than 30 MeV. For decay modes that include a π^0 , ΔE is required to satisfy $-50 \text{ MeV} < \Delta E < 30 \text{ MeV}$. To eliminate slow π^0 backgrounds, the angle of the kaon with respect to the K^* direction in the K^* rest frame, θ_{K^*} , is required to satisfy $\cos\theta_{K^*} < 0.8$. This is equivalent to a requirement that the π^0 momentum be greater than 175 MeV/c. When an event contains more than one candidate passing the above requirements, the combination for which ΔE is closest to zero is selected. Defining the signal region as $5.27 \text{ GeV}/c^2 < M_{bc} < 5.29 \text{ GeV}/c^2$, we find that the numbers of events passing the selection criteria and lying in the signal region are 968 for $J/\psi K^{*0}(K^+\pi^-)$, 241 for $J/\psi K^{*+}(K_S\pi^+)$, 220 for $J/\psi K^{*+}(K^+\pi^0)$ and 42 for $J/\psi K^{*0}(K_S\pi^0)$.

For each reconstructed mode, the distribution in M_{bc} is binned and fitted to a parameterized function of the form

$$N(M_{bc}) = f_{sig}(M_{bc}) + \sum_i f_{cf}^i(M_{bc}) + f_{nr}(M_{bc}) + f_{combi}(M_{bc}), \quad (1)$$

where f_{sig} , f_{cf}^i , f_{nr} , and f_{combi} are the shapes for the signal, background from other $B \rightarrow J/\psi K^*$ modes (which we will refer to as cross-feed), background from non-resonant $B \rightarrow J/\psi K\pi$, and combinatorial background, respectively. f_{sig} is a Gaussian with the peak position fixed at the B mass and a width that is determined from Monte Carlo. Only the amplitude is varied in fitting. f_{cf}^i is described by a separate Gaussian for each of the three $J/\psi K^*$ decay modes other than the signal mode. Monte Carlo simulations are used to determine the mean and width for each mode, as well as the efficiency for it to pass the signal mode criteria. The amplitudes of f_{cf}^i are scaled such that the ratios of cross-feed to signal efficiency are fixed assuming equal production rates and decay branching fractions for the neutral and charged B 's. The rate of cross-feed from $B \rightarrow J/\psi K$ modes is also estimated using Monte Carlo and found to be negligible. The total amount of the cross-feed is estimated to be 1.8–6.2% (depending on the mode) of the events in the signal region. The shape of f_{nr} is also assumed to be a Gaussian. While the mean and width are expected to be similar to those of f_{sig} , they are determined separately to allow for minor kinematic differences, using events in the K^* mass sideband ($1.1 \text{ GeV}/c^2 < M(K\pi) < 1.3 \text{ GeV}/c^2$). The magnitude of the non-resonant contribution is derived from fitting the $K\pi$ mass distribution for events selected by the criteria used for the signal reconstruction without requiring the $K\pi$ mass to be inside the K^* mass window. The $K\pi$ mass distribution (Fig. 1) is fitted with P-wave and D-wave Breit-Wigner functions describing the $K^*(892)$ and $K_2^*(1430)$ mass peaks, respectively, and a threshold function constrained at the mass threshold to describe the non-resonant production. The peak positions and widths of the Breit-Wigner functions are fixed to the nominal PDG values[5]. The amplitude of f_{nr} is determined from the contribution of the fitted background functions in the K^* mass that takes into

account the contamination of the combinatorial background in the functions. The estimated contribution of the non-resonant decay in the signal region is 5.2%. f_{combi} is the line shape for the combinatorial background and is modeled by the “ARGUS function” [6], where the parameters are free in the fit. Fig. 2 shows the results of the fits to four modes. The fits indicate the contamination of the combinatorial background is less than 1% in the signal region.

The branching fraction is calculated from the yield in the signal region obtained from the fitted f_{sig} . The detection efficiency for each mode is estimated by applying the selection criteria to Monte Carlo event samples. Events are generated unpolarized in the $J/\psi K^*$ system using the QQ event generator [7] and are passed through a detector simulation program based on GEANT3 [8]. The estimated efficiencies are 28.4%, 20.7%, 11.8%, and 8.1%, for $J/\psi K^{*0}(K^+\pi^-)$, $J/\psi K^{*+}(K_S\pi^+)$, $J/\psi K^{*+}(K^+\pi^0)$ and $J/\psi K^{*0}(K_S\pi^0)$, respectively. The branching fractions of secondary decays are fixed to the PDG values [5] and the numbers of neutral and charged $B\bar{B}$ pairs from $\Upsilon(4S)$ decays are assumed to be equal.

The systematic uncertainties on the branching fractions are dominated by the following sources: 1) tracking efficiency (2.0% per track), 2) π^0 reconstruction (3.0%), 3) lepton identification efficiency (5.0%), 4) kaon identification efficiency ($< 1.0\%$), 5) background estimation (2.3–4.8% depending on the mode), 6) number of $B\bar{B}$ events (1.0%), 7) polarization (1.7%), and 8) branching fraction for secondary decays (1.7%). The estimate of the non-resonant $B \rightarrow J/\psi K\pi$ background has a relatively large uncertainty because the fit to the $K\pi$ mass distribution is poor in the region of $K\pi$ mass from 1.1 GeV/ c to 1.3 GeV/ c , where some excess is observed. This excess has also been seen elsewhere [9,10], and there has been some speculation as to its origin [9]. As its source is not established, we estimate the uncertainty in its contribution to the signal by including in the fit to the $K\pi$ mass distribution an additional term that is constrained to zero at the mass threshold and extends linearly to 1.35 GeV/ c^2 . The change to the signal yield due to this modification is taken to be the uncertainty.

The resulting branching fractions are summarized in Table 1 with the estimated systematic errors.

4 Measurement of decay amplitudes

The decay amplitudes of $B \rightarrow J/\psi K^*$ decays are measured in the transversity basis [11]. The direction of motion of the J/ψ in the rest frame of the B candidate is defined to be the x -axis. The y -axis is defined to be in the direction of the projection of the K momentum into the plane perpendicular to the

x -axis in the B rest frame. The x - y plane contains the momenta of the J/ψ , the K , and the π . The z -axis is defined to be perpendicular to the x - y plane according to the right-hand rule. The angle between the l^+ direction and the z -axis in the J/ψ rest frame is defined as θ_{tr} . The angle between the x -axis and the projection of the l^+ momentum onto the x - y plane is defined as ϕ_{tr} in the same frame. The angle θ_{K^*} is defined as described in the previous section.

The distribution of these three angles for $B \rightarrow J/\psi K^*$ decays is described in terms of three amplitudes[12]:

$$\begin{aligned} \frac{1}{\Gamma} \frac{d\Gamma}{d \cos \theta_{tr} d \cos \theta_{K^*} d \phi_{tr}} = & \frac{9}{32\pi} \times [2 \cos^2 \theta_{K^*} (1 - \sin^2 \theta_{tr} \cos^2 \phi_{tr}) |A_0|^2 \\ & + \sin^2 \theta_{K^*} (1 - \sin^2 \theta_{tr} \sin^2 \phi_{tr}) |A_{\parallel}|^2 \\ & + \sin^2 \theta_{K^*} \sin^2 \theta_{tr} |A_{\perp}|^2 \\ & + \eta \sin^2 \theta_{K^*} \sin 2\theta_{tr} \sin \phi_{tr} \text{Im}(A_{\parallel}^* A_{\perp}) \\ & - \frac{1}{\sqrt{2}} \sin 2\theta_{K^*} \sin^2 \theta_{tr} \sin 2\phi_{tr} \text{Re}(A_0^* A_{\parallel}) \\ & + \eta \frac{1}{\sqrt{2}} \sin 2\theta_{K^*} \sin 2\theta_{tr} \cos \phi_{tr} \text{Im}(A_0^* A_{\perp})], \quad (2) \end{aligned}$$

where A_0 , A_{\parallel} and A_{\perp} are the complex amplitudes of the three helicity states in the transversity basis, and $\eta = +1$ (-1) for B^0 and B^+ (\bar{B}^0 and B^-). $|A_0|^2$ denotes the longitudinal polarization of J/ψ while $|A_{\perp}|^2$ ($|A_{\parallel}|^2$) is the transverse polarization component along the z -axis (y -axis). Also, $|A_0|^2 + |A_{\parallel}|^2$ is the amplitude corresponding to the CP-even state, while $|A_{\perp}|^2$ is the CP-odd component in $B^0 \rightarrow J/\psi K^{*0}$ ($K^{*0} \rightarrow K_S \pi^0$). These amplitudes are normalized so that:

$$|A_0|^2 + |A_{\parallel}|^2 + |A_{\perp}|^2 = 1. \quad (3)$$

The amplitudes are determined by fitting this function to the measured three-dimensional distribution in θ_{tr} , ϕ_{tr} and θ_{K^*} , taking into account the detection efficiency and background. The resolution of the angular measurements is estimated by Monte Carlo and found to be typically less than 0.02 radians. The value of η is determined from the charge of pions or kaons used in the K^* reconstruction. We do not include the $B^0 \rightarrow J/\psi K^{*0}(K_S \pi^0)$ mode in the fit since in this case η is not well-defined.

The fit is performed using an unbinned maximum likelihood method. The probability density function (PDF) is defined using the theoretical distribution in (2) and can be expressed as

$$\begin{aligned}
PDF(x, y, z, M_{bc}) = & N \times [f_{sig}(M_{bc}) \times \epsilon(x, y, z) \times \frac{1}{\Gamma} \frac{d^3\Gamma}{dx dy dz}(x, y, z) \\
& + \sum_i f_{cf}^i(M_{bc}) \times ADF_{cf}(x, y, z) \\
& + f_{nr}(M_{bc}) \times ADF_{nr}(x, y, z) \\
& + f_{combi}(M_{bc}) \times ADF_{combi}(x, y, z)], \tag{4}
\end{aligned}$$

where $x = \cos\theta_{tr}$, $y = \phi_{tr}$, and $z = \cos\theta_{K^*}$, N is the normalization factor of the PDF, $\epsilon(x, y, z)$ is the detection efficiency as a function of the three angles, and ADF_{cf} , ADF_{nr} , ADF_{combi} are the angular shapes for the cross-feed, non-resonant and combinatorial backgrounds, respectively.

Here, $f_{sig}(M_{bc})$, $f_{cf}^i(M_{bc})$, $f_{nr}(M_{bc})$, and $f_{combi}(M_{bc})$ are the fractions of signal events, cross-feed contamination, non-resonant contamination and combinatorial background as a function of beam constrained mass, respectively. These fractions are obtained from the measurements of the branching fractions described in the previous section.

The detection efficiency function $\epsilon(x, y, z)$ is obtained from a large Monte Carlo sample of 1 million events for each mode generated without any polarization of the $B \rightarrow J/\psi K^*$ system. Events are histogrammed in a $20 \times 20 \times 20$ grid in a $\cos\theta_{tr} - \phi_{tr} - \cos\theta_{K^*}$ cube. The distribution is fitted to a three-dimensional polynomial with correlations taken into account. The efficiency is almost flat except in the region $\cos\theta_{K^*} \sim 1$, where the pion is slow so that the efficiency is reduced.

The angular distribution function for the cross-feed background (ADF_{cf}) is determined from the distribution in Monte Carlo events. The function for the non-resonant production (ADF_{nr}) is determined from events in the sideband of the $K\pi$ mass distribution. The distribution for the combinatorial background (ADF_{combi}) is obtained from events in the sideband of the beam-constrained mass. These distributions are parameterized as polynomials where the parameters are determined from the fit.

In the fit to the angular distributions, the imaginary part of A_0 is defined to be zero relative to the imaginary parts of the other amplitudes since the overall phase of the decay amplitudes is arbitrary. By applying the normalization condition (3), four parameters, $|A_0|^2$, $|A_\perp|^2$, $\arg(A_\parallel)$ and $\arg(A_\perp)$ are left to be determined from the fit. The normalization of the PDF (N) is calculated by numerical integration over the three dimensional angular cube whenever parameter values are changed. A likelihood is defined as the product of the PDF for all the events and the values of parameters are determined by maximizing the likelihood. We perform separate fits to the three decay modes as well as a combined fit by defining a single likelihood. The parameter values determined from these fits are summarized in Table 2. The projected angular distributions

of the data for all K^* modes combined are shown in Fig. 3. The distributions are corrected for the effects of detector acceptance and backgrounds.

Systematics in the fit are studied for the following uncertainties: 1) efficiency function (Monte Carlo statistics and effect of polarization), 2) angular distribution functions for backgrounds, 3) background fractions, 4) slow pion efficiency, and 5) fit algorithm. These contributions to the systematic error are summarized in Table 3. The dominant contributions arise from the dependence of the efficiency and background functions on the polarization, and also the uncertainty in the detection efficiency for slow pions. The first uncertainty is estimated by comparing the functions obtained for Monte Carlo samples generated with and without the polarization in the $J/\psi K^*$ system. The second uncertainty dominates in the $\cos \theta_{K^*}$ distribution where $\cos \theta_{K^*}$ is close to 1. The uncertainty is estimated by comparing with the results with a cut at $\cos \theta_{K^*} < 0.9$ for decay modes with π^\pm and with a cut at $\cos \theta_{K^*} < 0.7$ for the mode with π^0 . The systematics in the fit algorithm are studied using toy Monte Carlo events. The differences between input decay amplitudes for Monte Carlo and the values obtained by the fit are taken as the uncertainties.

5 Conclusion

Branching fractions for $B^0 \rightarrow J/\psi K^{*0}$ and $B^+ \rightarrow J/\psi K^{*+}$ are measured via reconstruction of $K^{*0} \rightarrow K^+\pi^-$, $K^{*0} \rightarrow K_S\pi^0$, $K^{*+} \rightarrow K^+\pi^0$, and $K^{*+} \rightarrow K_S\pi^+$ with leptonic decays of J/ψ . The resultant branching fractions are $Br(B^0 \rightarrow J/\psi K^{*0}) = (1.29 \pm 0.05 \pm 0.13) \times 10^{-3}$ and $Br(B^+ \rightarrow J/\psi K^{*+}) = (1.28 \pm 0.07 \pm 0.14) \times 10^{-3}$. These values are consistent with the measurements by CLEO[10] and BaBar[13] (Table 4).

The decay amplitudes for $B \rightarrow J/\psi K^*$ are measured by fitting the angular distribution of final state particles in the transversity basis to a theoretical distribution with the effects of the detector acceptance and the background taken into account. In the fit, the sum of amplitudes is normalized to 1 ($|A_0|^2 + |A_\parallel|^2 + |A_\perp|^2 = 1$) and $\arg(A_0)$ is defined to be zero. The fit is performed using an unbinned maximum likelihood method. From the fit, the values obtained are $|A_0|^2 = 0.618 \pm 0.020 \pm 0.027$, $|A_\perp|^2 = 0.191 \pm 0.023 \pm 0.026$, $\arg(A_\parallel) = 2.83 \pm 0.19 \pm 0.08$, and $\arg(A_\perp) = -0.09 \pm 0.13 \pm 0.06$. The measured value of $|A_\perp|^2$ shows that the CP even component dominates in the decay $B^0 \rightarrow J/\psi K^{*0}(K_S\pi^0)$. The value is used in the determination of $\sin 2\phi_1$ as described in [1]. Table 5 shows the comparison with other measurements. The parameter $\arg(A_\parallel)$ is sensitive to final state interactions (FSI). A shift from 0 or π shows the existence of the FSI. The measured value is consistent with results from other experiments[9][14]. However, the significance of its deviation from π is not sufficient to conclude the existence of FSI.

We wish to thank the KEKB accelerator group for the excellent operation of the KEKB accelerator. We acknowledge support from the Ministry of Education, Culture, Sports, Science, and Technology of Japan and the Japan Society for the Promotion of Science; the Australian Research Council and the Australian Department of Industry, Science and Resources; the National Science Foundation of China under contract No. 10175071; the Department of Science and Technology of India; the BK21 program of the Ministry of Education of Korea and the CHEP SRC program of the Korea Science and Engineering Foundation; the Polish State Committee for Scientific Research under contract No. 2P03B 17017; the Ministry of Science and Technology of the Russian Federation; the Ministry of Education, Science and Sport of the Republic of Slovenia; the National Science Council and the Ministry of Education of Taiwan; and the U.S. Department of Energy.

References

- [1] K.Abe *et al.* (Belle Collaboration), “Observation of Mixing-induced CP Violation in the Neutral B Meson System”, hep-ex/0202027 (2002), submitted to Phys. Rev. D; K.Abe *et al.* (Belle Collaboration), Phys. Rev. Lett. **87**, 091802 (2001).
- [2] A.Abashian *et al.* (Belle Collaboration), Nucl. Inst. and Meth. **A479**, 117 (2002).
- [3] E. Kikutani ed., KEK Preprint 2001-157 (2001), to appear in Nucl. Inst. and Meth. **A**.
- [4] G.Fox and S.Wolfram, Phys. Rev. Lett **41**, 1581 (1978).
- [5] D.E.Groom *et al.* (Particle Data Group), Eur. Phys. J. **C15**, 1 (2000).
- [6] H.Albrecht *et al.*, Phys. Lett. B **241**, 278 (1990).
- [7] See <http://www.lns.cornell.edu/public/CLEO/soft/QQ/>.
- [8] R.Brun *et al.*, GEANT 3.21, CERN Report No. DD/EE/84-1 (1987).
- [9] B.Aubert *et al.* (BaBar Collaboration), Phys. Rev. Lett. **87**, 241801 (2001).
- [10] C.S.Jessop *et al.* (CLEO Collaboration), Phys. Rev. Lett. **79**, 4533 (1997); CLEO Collaboration, CLEO CONF 96-24 (1996).
- [11] I.Dunietz, H.Quinn, A.Snyder, W.Toki and H.J.Lipkin, Phys. Rev. D **43**, 2193 (1991).
- [12] K.Abe, M.Satpathy and H.Yamamoto, “Time-dependent angular analysis of B decays”, hep-ex/0103002 (2001).
- [13] B.Aubert *et al.* (BaBar Collaboration), Phys. Rev. D **65**, 032001 (2002).
- [14] T.Affolder *et al.* (CDF Collaboration), Phys. Rev. Lett. **85**, 4668 (2000).

Table 1

Measured branching fractions for $B^0 \rightarrow J/\psi K^{*0}$ and $B^+ \rightarrow J/\psi K^{*+}$.

Mode	Branching Fraction ($\times 10^{-3}$)
$B^0 \rightarrow J/\psi K^{*0}(K^+\pi^-)$	$1.30 \pm 0.05 \pm 0.12$
$B^0 \rightarrow J/\psi K^{*0}(K_S\pi^0)$	$1.20 \pm 0.20 \pm 0.15$
$B^0 \rightarrow J/\psi K^{*0}$	$1.29 \pm 0.05 \pm 0.13$
$B^+ \rightarrow J/\psi K^{*+}(K_S\pi^+)$	$1.23 \pm 0.11 \pm 0.15$
$B^+ \rightarrow J/\psi K^{*+}(K^+\pi^0)$	$1.33 \pm 0.10 \pm 0.14$
$B^+ \rightarrow J/\psi K^{*+}$	$1.28 \pm 0.07 \pm 0.14$

Table 2

Measured decay amplitudes for $B^0 \rightarrow J/\psi K^{*0}$ and $B^+ \rightarrow J/\psi K^{*+}$ (statistical error only).

Mode	$ A_0 ^2$	$ A_\perp ^2$	$arg(A_\parallel)$	$arg(A_\perp)$
$B^0 \rightarrow J/\psi K^{*0}(K^+\pi^-)$	0.607 ± 0.020	0.195 ± 0.023	2.87 ± 0.19	0.04 ± 0.13
$B^+ \rightarrow J/\psi K^{*+}(K_S\pi^+)$	0.630 ± 0.048	0.171 ± 0.057	2.74 ± 0.39	-0.45 ± 0.33
$B^+ \rightarrow J/\psi K^{*+}(K^+\pi^0)$	0.653 ± 0.052	0.194 ± 0.087	2.69 ± 1.08	-0.23 ± 0.56
Combined	0.617 ± 0.020	0.192 ± 0.023	2.83 ± 0.19	-0.09 ± 0.13

Table 3

Systematic errors in the measurement of decay amplitudes.

Item	$ A_0 ^2$	$ A_\perp ^2$	$arg(A_\parallel)$	$arg(A_\perp)$
Efficiency	0.008	0.003	0.04	0.03
ADF for backgrounds	0.007	0.003	0.01	0.04
Background fractions	0.001	0.001	0.01	0.01
Slow pion efficiency	0.025	0.026	0.07	0.02
Fit algorithm	0.001	0.001	<0.01	0.01
Total	0.027	0.026	0.08	0.06

Table 4

Comparison with previous measurements of branching fractions for $B^0 \rightarrow J/\psi K^{*0}$ and $B^+ \rightarrow J/\psi K^{*+}$. The first (second) quoted error is statistical (systematic).

	$Br(B^0 \rightarrow J/\psi K^{*0}) (\times 10^{-3})$	$Br(B^+ \rightarrow J/\psi K^{*+}) (\times 10^{-3})$
CLEO[10]	$1.32 \pm 0.15 \pm 0.17$	$1.41 \pm 0.20 \pm 0.24$
BaBar[13]	$1.24 \pm 0.05 \pm 0.09$	$1.37 \pm 0.09 \pm 0.11$
This measurement	$1.29 \pm 0.05 \pm 0.13$	$1.28 \pm 0.07 \pm 0.14$

Table 5

Comparison with previous measurements of decay amplitudes in $B \rightarrow J/\psi K^*$. The first (second) quoted error is statistical (systematic).

Group	$ A_0 ^2$	$ A_\perp ^2$	$arg(A_\parallel)$	$arg(A_\perp)$
CLEO[10]	$0.52 \pm 0.07 \pm 0.04$	$0.16 \pm 0.08 \pm 0.04$	$3.00 \pm 0.37 \pm 0.04$	$-0.11 \pm 0.46 \pm 0.03$
CDF[14]	$0.59 \pm 0.06 \pm 0.01$	$0.13^{+0.12}_{-0.09} \pm 0.06$	$2.2 \pm 0.5 \pm 0.1$	$-0.6 \pm 0.5 \pm 0.1$
BaBar[9]	$0.60 \pm 0.03 \pm 0.02$	$0.16 \pm 0.03 \pm 0.01$	$2.50 \pm 0.20 \pm 0.08$	$-0.17 \pm 0.16 \pm 0.07$
This measurement	$0.62 \pm 0.02 \pm 0.03$	$0.19 \pm 0.02 \pm 0.03$	$2.83 \pm 0.19 \pm 0.08$	$-0.09 \pm 0.13 \pm 0.06$

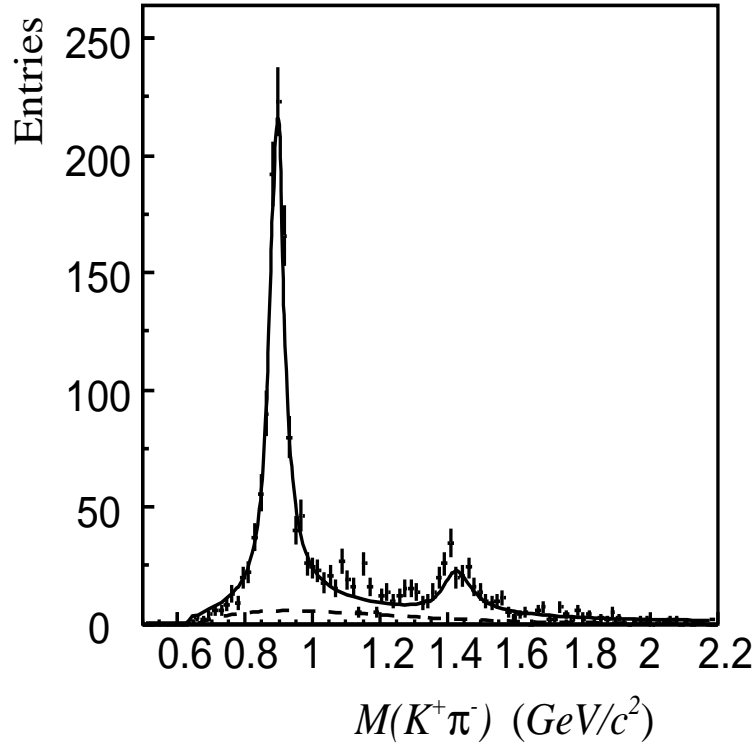


Fig. 1. The invariant $K\pi$ mass distribution for $B^0 \rightarrow J/\psi K^{*0}(K^+\pi^-)$ candidates. The solid line shows a fit to two Breit-Wigner functions corresponding to $K^*(892)$ and $K_2^*(1430)$ with a background function (dashed line).

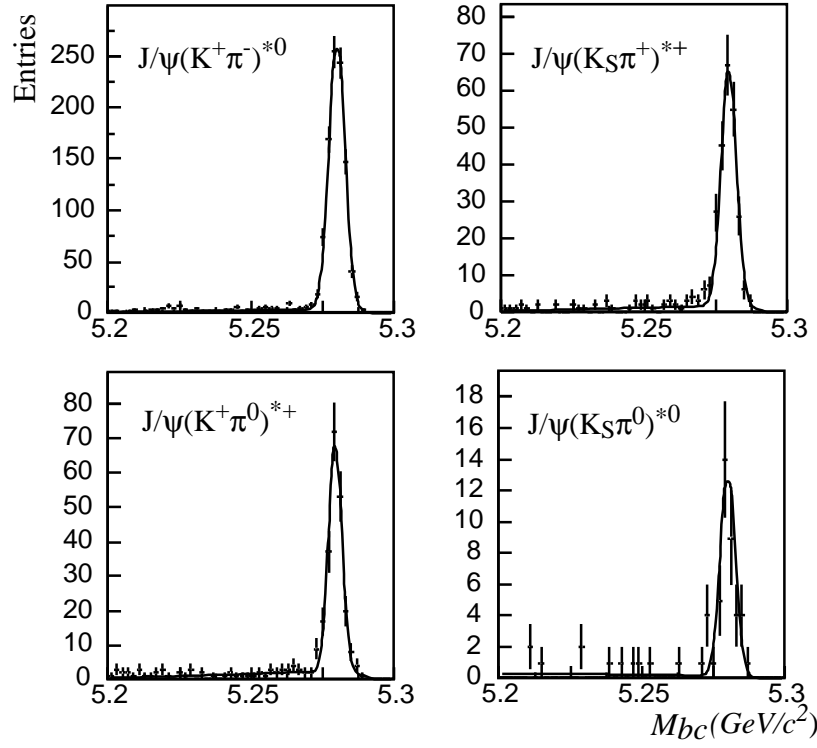


Fig. 2. The distributions of the beam-constrained mass for four reconstructed modes. The solid lines show the fits.

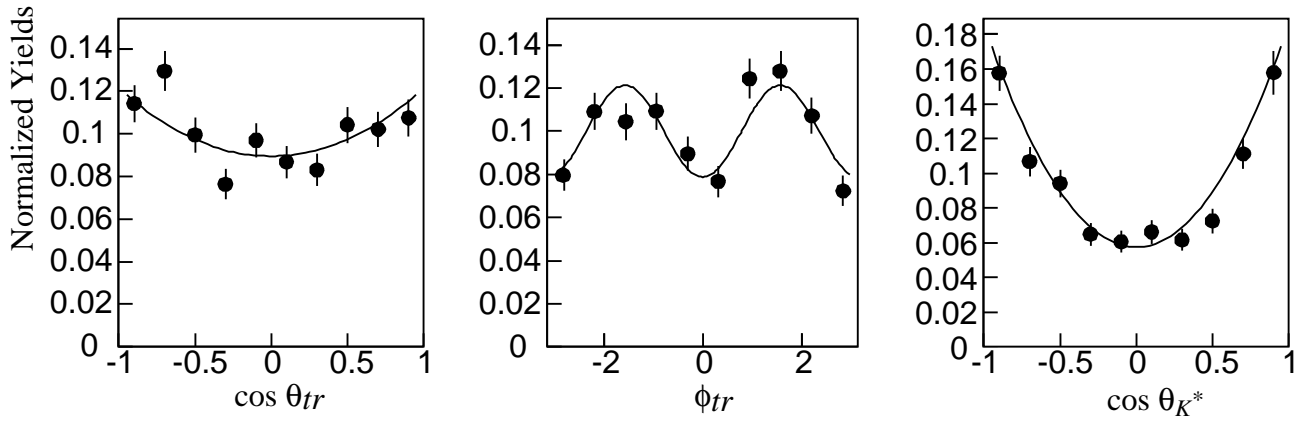


Fig. 3. Projected distributions of $\cos \theta_{tr}$, ϕ_{tr} and $\cos \theta_{K^*}$ for the combined data. The distributions are background subtracted and acceptance corrected. The solid line shows the theoretical predictions with the obtained decay amplitudes.